AIAA JOURNAL
Vol. 49, No. 3, March 2011

Flutter Failure Risk Assessment for Damage-Tolerant Composite Aircraft Structures

Andrey V. Styuart,* Eli Livne,† Luciano Demasi,‡ and Marat Mor§
University of Washington, Seattle, Washington 98195-2400

DOI: 10.2514/1.J050862

The quantitative assessment of the effects of damage and material degradation on the dynamic aeroelastic reliability of composite aircraft has become more challenging in recent years due to the increased use of composites in main structural components of passenger aircraft. This paper presents a method for quantifying the flutter reliability of aircraft composite structures in the presence of multiple uncertainties. Automated rapid simulation tools for predicting flutter speeds of composite airframes subject to multiple uncertainties serve a key role and are used in Monte Carlo simulations. A thorough discussion is presented of the flutter uncertainty of composite aircraft covering material degradation, damage, repair, and design and certification practices, as well as maintenance procedures. The effectiveness of the method and its potential are illustrated using a composite tail/rudder structure representing a typical passenger aircraft structure. Conclusions are drawn and recommendations for future work are made.

Nomenclature

$[A]$	=	time-domain state-space system matrix
$[A_0]$, $[A_1]$, $[A_2]$	=	unsteady aerodynamic force rational function approximation matrices
b	=	reference semichord
C_V	=	coefficient of variation
c	=	c.g. location of control surface behind its hinge line
$[D]$, $[E]$, $[R]$	=	matrices associated with lag terms in a rational function approximation of unsteady aerodynamic matrices
D_{VF}	=	variance of flutter speed of a fleet
D_X	=	variance of parameter x in a fleet
EI	=	spanwise distribution of wing bending stiffness
$F(V/V_D)$	=	cumulative frequency of airspeed occurrence (sometimes referred to as exceedance curve)
F_{Va}	=	cumulative probability distribution function of maximum random airspeed per life of a fleet of the same model airplane
F_{V_f}	=	joint cumulative probability distribution function of flutter speed in a fleet of the same airplane model
f_{VF}	=	probability density function of random flutter speed
$f_X(X\|Y)$	=	conditional probability density function (probability density of X when Y is known to be a particular value)
GJ	=	spanwise distribution of wing torsion stiffness
I_m	=	per unit span mass moment of inertia distribution
k	=	reduced frequency of oscillation
$[M]$, $[C]$, $[K]$	=	generalized mass, damping, and stiffness matrices, respectively
$[\bar{M}]$, $[\bar{C}]$, $[\bar{K}]$	=	generalized coupled structural-aerodynamic mass, damping, and stiffness matrices, respectively
m	=	per unit span mass distribution of a wing
N_f	=	number of flights per life
P_f	=	probability of failure
$[Q(jk)]$	=	Fourier-transformed aerodynamic generalized force coefficients matrix
q_D	=	dynamic pressure
V	=	flight speed
V_a	=	flight speed that exceeds flutter speed for a particular airplane
V_C/M_C	=	design cruise speed/Mach number as defined in Federal Aviation Administration regulations
V_D/M_D	=	design dive speed/Mach number as defined in Federal Aviation Administration regulations
$V_{\mathrm{DF}}/M_{\mathrm{DF}}$	=	demonstrated flight diving speed/Mach number as defined in Federal Aviation Administration regulations
V_{DFS}	=	design flutter speed
V_F	=	design flap speed as defined in Federal Aviation Administration regulations
V_f	=	flutter speed
$\bar{V}_f$	=	mean flutter speed of aircraft fleet
V_{fm}	=	flutter speed measured in flight tests
Vij	=	flutter speed of individual airplanes in fleet j
Vj	=	mean flutter speed of aircraft of model j
V_{MO}	=	airspeed limit as defined in the aircraft flight manual
W	=	total cross-sectional width of a panel
W_D	=	maximum cross-section of damage size normal to the direction of the applied load
X_{ij}	=	Vij/Vj flutter speed of individual airplane i in fleet j (used to quantify individual uncertainty)
X_{im}	=	$Vij\mathrm{test}/Vj$ when $Vij\mathrm{test}$ is a flutter speed of the ith article of fleet j measured in flight tests with some error
$x_{c.g.}$	=	position of wing station cross-section center of mass
Yj	=	Vj/Vj_{DES} mean flutter speed for a fleet of aircraft type j normalized by the design flutter speed for that fleet (used to quantify systemic uncertainty)

Received 12 August 2010; accepted for publication 7 September 2010.

*Acting Assistant Professor, Department of Aeronautics and Astronautics; currently Engineering Specialist, Stirling Dynamics, Inc., Kirkland, Washington.

†Professor, Department of Aeronautics and Astronautics. Associate Fellow AIAA.

‡Postdoctoral Research Fellow, Department of Aeronautics and Astronautics; currently Assistant Professor, San Diego State University, Department of Aerospace Engineering and Engineering Mechanics, San Diego, California.

§Postdoctoral Research Fellow, Department of Aeronautics and Astronautics; currently Engineering Manager and Principal Engineer, Stirling Dynamics, Inc., Kirkland, Washington.

$z \rightarrow V/V_D$ = normalized flight speed
β = shape parameter of probability distribution
$\kappa_{C(D)}$ = compressive stiffness of the damage region, which is negligible for hole
$\kappa_{C(U)}$ = original compressive stiffness of the composite,
$\kappa_{T(D)}$ = tensile stiffness of the damage region, which is negligible for hole,
$\kappa_{T(U)}$ = original tensile stiffness of the composite,
μ = scale parameter of probability distribution
σ_{VF} = standard deviation of flutter speed
σ_p = standard deviation of parameter
$\{\xi(j\omega)\}$ = generalized displacements used to determine the motion of an elastic airplane

I. Introduction

A METHODOLOGY for flutter risk assessment for damage-tolerant composite aircraft structures is presented in this paper. This development is motivated by the increased use of composite materials in civil aircraft structures. Current certification regulations [1] require that an airframe be designed so that its critical flutter speed/Mach number V_f/M_f will be greater by specified margins than the design dive speed/Mach number V_D/M_D of the aircraft to ensure its flutter safety. Critical flutter speeds V_f depend on a wide range of different structural parameters, including material properties, structural layout, dimensions of structural components, mass distribution, position of engines and their attachment method, mass balance of control surfaces, control system parameters, etc. (e.g., [2]). Damage at any locations of such complex structural systems may have a negative effect on overall flutter safety. As the use of composite materials in aircraft structures becomes more widespread with new structural layouts, joining techniques, corresponding material variability, damage characteristics, and repair and maintenance procedures, a greater need exists to develop methods for quantitative assessment of the probability of failure (POF) due to flutter. This will allow aircraft manufacturers, operators, and government authorities to develop appropriate design and maintenance procedures.

Work on the uncertainty and reliability of aeroelastic behavior has been presented in quite a number of publications ([2] is an excellent survey) and is still pursued worldwide. Most probabilistic aeroelastic studies to date involve very simple aeroelastic models, such as panels, two-dimensional airfoils, or simple wing boxes. To avoid the computational cost of Monte Carlo simulations, various probability integration and averaging methods have often been used. Also, due to the lack of statistical input data, consideration of the importance of various primitive random variables (consideration that can reduce simulations times and numbers) has usually been missing in most studies to date.

In the work presented here, concepts of reliability-based damage-tolerant structural design and maintenance methodology, presented in [3], are extended and applied to the case of flutter failure mechanisms. There are three major elements to the new tools developed. First, an adequate deterministic method for rapid assessment of flutter behavior must be in place and must be completely automated to provide flutter behavior characteristics for systems that are subject to parameter variations. Second, an adequate probabilistic method for assessment of the probability of flutter failure must be developed, assuming that statistical information on the important uncertainties is available. The method should be general so that it can be quickly adapted to cases of different levels of complexity, different types and scopes of statistical information, and different fundamental mechanisms involved. Finally, statistical sets of data on inherent uncertainties in composite airframes must be obtained and examined, and methodologies for collection and incorporation of such information must be developed.

The test case used in this paper is a representative three-dimensional finite element (FE)-based model of a composite tail/rudder system of a passenger airplane. The linear flutter simulation capability used here is completely automated to yield flutter speeds for any combination of system parameters used.

The paper is structured as follows. First, a computational simulation system developed for the rapid flutter analysis of multiple complex configurations subject to parameter uncertainties is described. A discussion of flutter speed uncertainty and its structural sources follows, taking into account systemic errors in the analysis and design methods used, as well as individual aircraft differences due to material property variability of aircraft in a fleet of the same model type. The effect of flutter flight tests on the resulting flutter speed distribution in a fleet are also discussed. The resulting flutter speed uncertainty estimates of aircraft are then combined with probabilistic information regarding the speeds at which such aircraft are actually flown to yield estimates of the probability of flutter failure of pristine aircraft (undamaged aircraft with no material degradation). The focus next shifts to the case of airplanes that are subject to material degradation, damage, damage detection, and damage repair over their lifetimes, and a methodology for assessing flutter reliability in such cases is presented. Results obtained using mathematical aeroelastic models of representative composite and metal airplanes are used to highlight the issues involved and offer some insight.

The problems addressed here are highly complex, and solid statistical data for various parameters involved are still incomplete, missing, or not openly reported. It is hoped that this paper will lead to procedures and efforts to collect such information. For the examples used here, every effort was made to use the best data openly available, with the understanding that with more complete fundamental data becoming available in the future, some of the results of the example problems used here may change.

II. Virtual Aeroelastic Testing Module: Automated Aeroelastic Simulation of Uncertain Damaged Airframes

An important building block in any numerical probabilistic reliability assessment system is the capability for efficiently and accurately carrying out numerical simulations of a large number of cases representing the system in its many variations. It is also important, since industry-level complexity and practice have to be covered in the methods development reported here, to base such simulation capability on widely accepted industry-standard simulation codes. The simulation array for FE-based models of aeroelastic systems used here [named the virtual aeroelastic testing module (VATM)] contains five modules connected through a network of interface programs to allow automated execution and output processing. Each new case simulated by this array evolves according to the block diagram shown in Fig. 1. A nominal FE model is created outside the loop shown so that it allows the adequate modeling of random thicknesses, materials, and damages by the changing properties of the FEs and corresponding material cards. In this model, it is expedient to have separate material cards and property cards for each FE. This model constitutes the basis for the FE model generator, which creates FE input decks to reflect the effects of damage and material property variations as required for Monte Carlo simulations of damage and material variations. Those variations are considered in detail later in the paper. The NASTRAN code [4] is then used to generate natural frequencies, natural mode shapes, generalized mass, and generalized stiffness matrices. Unsteady aerodynamics panel codes, such as doublet lattice or ZAERO [5] use this NASTRAN output to generate generalized force aerodynamic coefficient matrices for a number of tabulated reduced frequencies covering the reduced frequency range of interest.

This is done (for given Mach numbers and reduced frequencies) by first calculating aerodynamic influence coefficients (AICs) on the aerodynamic mesh and then proceeding to calculate generalized aerodynamic forces for a set of modes using interpolation between the aerodynamic mesh and the structural grid on which the modes are defined. We consider damage and material degradation in this exploratory study where the planform shape does not change. Effects of planform, static deformation, and unsteady AIC uncertainties can be added later using unsteady aerodynamic sensitivities [6,7] or AIC reanalysis to accelerate the reanalysis of the unsteady aerodynamic loads. With aeroelastic uncertainty limited to structural material and

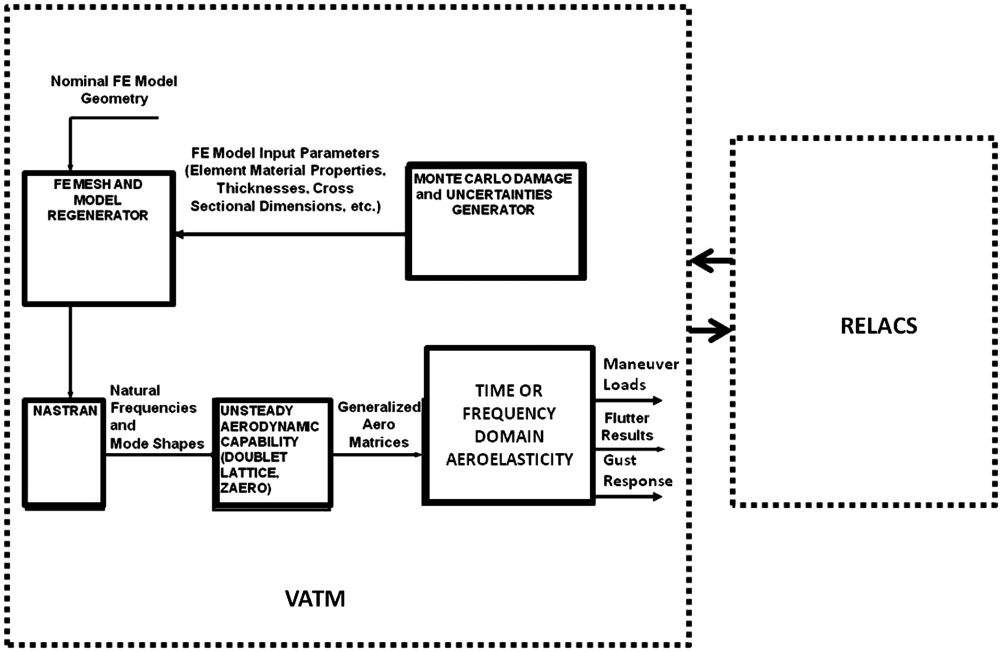

Fig. 1 VATM: automated system for simulating aeroelastic behavior as a function of variations in system structural parameters.

sizing variations, and since the AICs are not affected by such changes, the AICs are calculated once per Mach number and reduced frequency and stored to be used repeatedly for generalized force matrix generation with different sets of mode shapes.

The method development and studies reported in the present paper focus on uncertain flutter behavior, and the linear aeroelastic problem in this case is formulated in the frequency domain as follows:

$$(-\omega^2[M] + j\omega[C] + [K] - q_D[Q(jk, M_\infty)])\{\xi(j\omega)\} = 0 \quad (1)$$

where $[Q(jk)]$ is the Fourier-transformed aerodynamic generalized force coefficients matrix, the matrices $[M]$, $[C]$, and $[K]$ are generalized mass, viscous damping, and stiffness matrices, respectively, q_D is dynamic pressure, M_∞ is the Mach number, ω is the oscillation frequency, and k is the reduced frequency. The vector of generalized structural dynamic motions using some modal base is $\{\xi(j\omega)\}$.

The automation of flutter response predictions for cases involving large model variations is not trivial [8–15]. In the linear case, when flutter speeds are sought, robust root tracking and interpolation algorithms are required in order to reliably follow the evolution of solution branches as functions of dynamic pressure and to overcome challenges posed by mode switching and interpolation errors.

A few methods are available for calculation of flutter speed in the frequency domain, such as the k, p-k, and g methods. The linear flutter results, however, are sensitive to the extrapolation and interpolation techniques used for mode tracking. Failure of the tracking process is encountered from time to time when system variations lead to complex mode switching during the flutter solution process. Differences in the interpolation of modal branches to find axis crossing precisely and the resulting effect on predicted flutter speeds can also obscure the actual perturbation due to small system parameter changes. If sensitivity analysis is used to construct Taylor-series-based approximations of flutter speed behavior, obtaining such sensitivities by finite differences can lead to inaccuracy due to the effect of branch crossing interpolation errors. Analytic deterministic flutter sensitivities are thus preferable in this case [14]. The term deterministic sensitivity is used here to distinguish it from probabilistic sensitivity, and it denotes the derivative of a deterministic system behavior measure with respect to any system parameter.

When a time-domain approach to flutter speed determination is used [16–23], the Roger or minimum-state fitting of rational function approximations (as functions of reduced frequency) to the frequency-dependent aerodynamic matrices is carried out:

$$[Q(jk)] \approx [\bar{Q}(jk)] = [A_0] + jk[A_1] + (jk)^2[A_2] + jk[D](jk[I] + [R])^{-1}[E] \quad (2)$$

This leads to a linear-time-invariant state-space model for the aeroelastic system. In Eq. (2), $[\bar{Q}(jk)]$ is the approximated aerodynamic generalized force coefficients matrix obtained by fitting a rational function of reduced frequency to the tabulated matrices provided by the unsteady aerodynamic code, and k is the reduced frequency of oscillation:

$$k = \frac{\omega b}{V} \quad (3)$$

The matrices $[A_0]$, $[A_1]$, $[A_2]$, $[D]$, $[E]$, and $[R]$ are constant real matrices, with $[R]$ being a positive diagonal matrix containing the roots of the aerodynamic lag terms. Gradient-based optimization or least-squares fitting procedures are used to match the rational approximation to the tabulated data in the frequency domain. A linear-time-invariant state-space model of the system in the time and Laplace domains,

$$\{\dot{x}(t)\} = [A]\{x(t)\} \Leftrightarrow s\{X(s)\} = [A]\{X(s)\} \quad (4)$$

is created, where a new state vector in the time (or Laplace) domain is defined as follows:

$$\{x(t)\}^T = \{\, \xi(t) \quad \dot{\xi}(t) \quad x_{\text{lag}}(t) \,\} \Leftrightarrow \{X(s)\}^T = \{\, \Xi(s) \quad s\Xi(s) \quad X_{\text{lag}}(s) \,\} \quad (5)$$

and the system's matrix is

$$[A] = \begin{bmatrix} [0] & [I] & [0] \\ -[\bar{M}]^{-1}[\bar{K}] & -[\bar{M}]^{-1}[\bar{C}] & q_D[\bar{M}]^{-1}[D] \\ [0] & [E] & \frac{V}{b}[R] \end{bmatrix} \quad (6)$$

with

$$[\bar{M}] = [M] - q_D\left(\frac{b}{V}\right)^2[A_2]; \qquad [\bar{C}] = [C] - q_D\frac{b}{V}[A_1]$$
$$[\bar{K}] = [K] - q_D[A_0] \quad (7)$$

In Eq. (5), $\{x_{\text{lag}}(t)\}$ is the vector of aerodynamic states that, in the time and Laplace domains, is given by

$$\{X_{\text{lag}}(s)\} = \left([I]s - \frac{V}{b}[R]\right)^{-1} s[E]\{\Xi(s)\}$$

$$\Leftrightarrow \{\dot{x}_{\text{lag}}(t)\} = \frac{V}{b}[R]\{x_{\text{lag}}(t)\} + [E]\{\dot{\xi}(t)\} \tag{8}$$

The dimension of the vector of aerodynamic lag states varies between n_{lag} for the minimum-state method and $n_{\text{lag}} \times n$ for the Roger approximation, where n_{lag} is the number of aerodynamic lag terms, and n is the number of generalized coordinates.

Flutter speeds can now be automatically evaluated in two ways using the time-domain model. When the eigenvalues of the system matrix in Eq. (6) are used, dynamic pressure is increased (consistent with Mach number) and eigenvalues are repeatedly evaluated. A response function of dynamic pressure (matched point solutions) defined by $\boldsymbol{f(q_D)}$ is tracked, where $\boldsymbol{f(q_D)}$ is the largest real part of any of the eigenvalues. When this function switches from negative to positive, the system becomes unstable. The values of dynamic pressure, before and after this switch occurs, can now be used to bracket the flutter point, and a one-dimensional golden-section algorithm [23] is used to zoom in on the flutter dynamic pressure to any desired accuracy. The initial dynamic pressure step size and limits must be set, of course, so as not to miss the first eigenvalue to make the first imaginary axis crossing. Note that a similar technique can be used with the k, p-k, and g methods to find flutter speed and frequency in an automated way. The root locus technique based on Eq. (4), however, is consistent with a different approach, in which the dynamic system [Eq. (4)] is excited repeatedly at gradually increasing dynamic pressures by exciting all the modes at time zero, and the state-space equations are integrated in time. Allowing for a few cycles of initial transient response and focusing on subsequent longer-term behavior, an automated algorithm counts peaks as a function of time and determines whether the response over time is convergent or divergent. Once divergent oscillations have been detected, dynamic pressure is systematically reduced until the flutter dynamic pressure is determined by the desired accuracy corresponding to simple harmonic motion. Note that the time-domain method can be used to add dynamic gust cases to the reliability analysis (not covered in the presentation here but an important element in determining aeroelastic reliability) and also to identify LCO cases when nonlinear aeroelastic systems are studied [24]. VATM, the automated flutter prediction capability developed for the studies presented here, can be used (based on user selection) to provide flutter speed prediction by frequency domain or time-domain methods described previously.

With a relatively small set of modes (even up to the order of 100) the procedures, with the computational speeds of today's computers, are very fast. To simulate many cases involving different variations of the structure, parallel processing can also be used effectively. The flutter speed results are now fed into a Monte Carlo uncertainty and damage generator module (Fig. 1), where uncertainties are evaluated and new cases are generated for new flutter calculations, closing the loop. Both structural uncertainty cases, the case of the as-built airplane and the case of airplanes sustaining damage and material changes during their service life, will be covered later in the paper. The process is completely automated and reliable. With the automated simulation capabilities described previously, the stage is now set for statistical studies of structural variability, damage, and material degradation effects on the linear flutter of composite airframes.

III. Probabilistic Considerations

A. General Approach

According to Federal Aviation Regulation (FAR) 25.629 [1], airplanes must be designed to be free from aeroelastic instability for all configurations and design conditions within the V_D/M_D versus altitude envelope, expanded at all points by an increase of 15% in equivalent airspeed at both constant Mach number and constant altitude. This can be considered a safety factor of 1.15 [1.2 for FAR 23], and it has to be met deterministically by covering all possible configurations and variations of a particular airplane, including accounting for failure in certain critical areas such as control surface hinges.

When the flutter speed V_f is treated as a random variable having different values for each aircraft in a fleet of some aircraft model (B-767, MD-82, etc.), the statistical characteristics of V_f depend on fleetwide statistical characteristics of the determining parameters. That is, an airplane model will have some distribution of flutter speed characteristics throughout the fleet, as airplanes of the same model can still be structurally different from one another, and throughout service life, as airframes over time may be subject to changes due to material degradation and damage.

With a distribution of flutter speeds for given airplane models on one hand, it is important to remember, on the other hand, that airplanes are not operated and flown uniformly and that in-service experience shows that the maximum per-life value of actual airspeed flown for a given model can also be slightly different for different fleet members. It may be less than or greater than the airspeed stipulated by the airworthiness regulations. Consequently, the maximum airspeed flown by a particular airplane over its service life can also be considered as a random variable.

The question now becomes: What is the probability that, in a fleet of a certain model, a member of the fleet with flutter characteristics that have changed due to material degradation and damage will find itself flying above the flutter speed of its current condition with the consequent flutter failure?

In the following discussion, we first focus on pristine airplanes for which the dynamic properties are constant over their lifetime. That is, we consider one value of flutter speed of a random aircraft and one value of maximum per-life airspeed for this aircraft (the case of varying flutter speeds over life in service will be discussed later in the paper). These are compared across the fleet and the events of the flight airspeed of operation Va exceeding the flutter speed. V_f (resulting in flutter failure) are recorded. After making such a comparison for N aircraft of the fleet (with N large enough) and finding that the flutter exceedance event has happened M times, we can evaluate the POF as $P_f = M/N$.

The POF due to flutter for the fleet can also be expressed as

$$P_f = 1 - \int_0^\infty F_{V_a}(V) f_{V_f}(V)\,\mathrm{d}V \tag{9}$$

where F_{Va} is a cumulative probability distribution function (CDF) of the maximum random airspeed V per life, and f_{Vf} is a probability density function (PDF) of the random flutter speed.

Of major importance, of course, are the following questions:

1) Given airplane design, construction, certification, operation, and maintenance technologies, what kind of statistical variability exists among airplanes of the same model in a fleet?

2) What kind of structural variability can be expected for the same vehicle over its lifetime?

Results relevant to the second question of repeated modal tests conducted during the fatigue tests of a full-scale metal aircraft structure are discussed in [25]. It is reported there that the appearance of cracks and subsequent structural repair in such structural components as wing, empennage, and fuselage did not change the two to four lowest symmetric modes within the accuracy of the modal tests. The change of natural frequencies measured after completion of full time fatigue tests did not exceed 2% of the initial values, and this could be considered as a practical invariance of those dynamic characteristics. This explains the fact that some studies consider the minimum flutter speed for an airplane to be invariable over its lifetime. For a primary metal structure of aircraft without major damage, Eq. (9) may be used for POF evaluation and, for that, the CDF of operational flight speed and the PDF of flutter speed distribution in a fleet must be known. We will later discuss the case of airplanes for which the structural dynamic properties may vary during their lifetimes.

The next section will focus on the statistics of operational flight speeds.

B. Statistics of Extreme Airspeeds of Operation

FAR documents consider several causes of exceeding the maximum airspeed for commercial aircraft types. These are uncontrolled dive, atmospheric variations (such as horizontal gusts and penetration of jet streams and cold fronts), instrument errors, and airframe production variations. Since it is natural to use the design airspeed (value of maximum allowed speed V_D) as a scaling reference for flight speeds, the ratio V/V_D will be used for the analysis of the statistical characteristics of airspeed exceedances. Considering the causes of possible exceedance of the maximum airspeed, human and instrumental errors are usually described by Gauss PDFs, and high gusts are described by exponential distributions (see FAR 25, appendix G [1]). It is shown in [25] that, in this situation, the frequency of occurrence of high speeds $V > 0.8V_D$ can be approximated by an exponential function. Such characteristics had been obtained previously for military aircraft by Taylor [26], and [27] uses an exponential form of the exceedance curve (cumulative frequency of occurrence). The PDF of the maximum flight airspeed per aircraft life has been described by the extreme value type I (Gumbel) distribution function:

$$G(V/V_D|\mu,\beta) = e^{-e^{(V/V_D-\mu)/\beta}} \tag{10}$$

The method of moments may be used to obtain the Gumbel shape β and scale μ parameters from the mean value and standard deviation:

$$\beta = \frac{\sigma\sqrt{6}}{\pi}; \qquad \mu = \bar{x} - 0.5772\beta \tag{11}$$

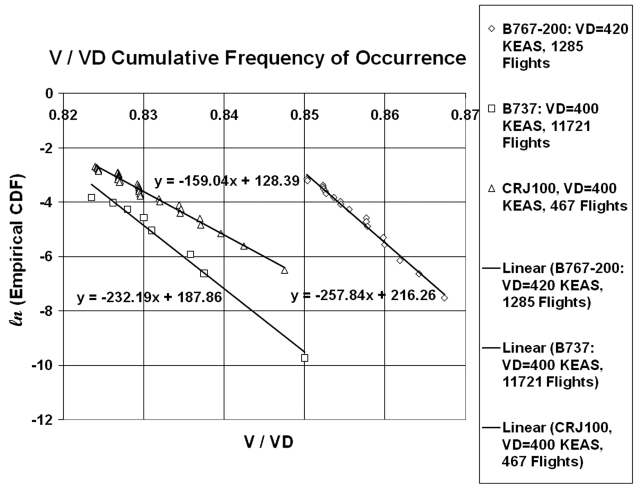

Fig. 2 Airspeed exceedance curve approximations (KEAS denotes the knots equivalent speed).

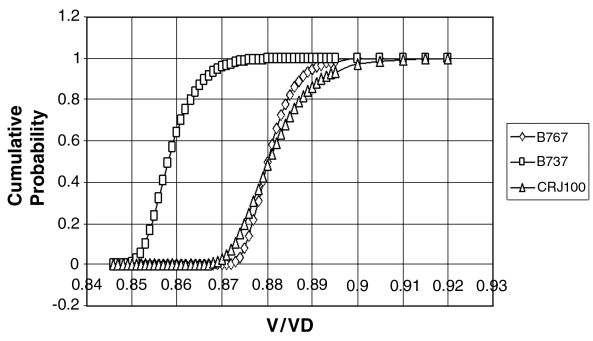

Fig. 3 CDF of maximum airspeed per 50,000 flight hours in flaps-retracted configuration.

Table 1 Data used to obtain F_{Va}

	B767	B737	CRJ100
Flights, N_f	7011.13	30,675.22	38,455.20
Hours	50,000.00	50,000.00	50,000.00
μ	0.838737	0.809079	0.807281
β	0.003878	0.004307	0.006288

The ranges of parameters β and μ, obtained for six maneuverable aircraft in [25], are $\beta = 0.045$ to 0.058 and $\mu = 0.95$ to 1.05 per service life. The shape of the PDF and its parameters for heavy commercial planes may, of course, be quite different from maneuverable aircraft.

Recent studies supported by the Federal Aviation Administration (FAA) made statistical data for passenger aircraft airspeeds available [28–32]. Unfortunately, this information is not organized as well as load factor or gust data information, and exceedance curves for airspeeds have not been presented. For the present work, we counted the dots on the charts that present the maximum per flight airspeeds that are to the right side of the different airspeed value; thus, the curves of the frequency of exceeding various airspeed levels per one flight (exceedance curve) were obtained. Figure 2 shows the most important right tails of probability of relative airspeed exceedance per one flight for three airplanes [28–32]. The linear interpolation functions are also shown. The CDF F_{Va} for Eq. (9) may be obtained from the exceedance curve by an asymptotic formula:

$$F_{Va}(V/V_D) = \exp\{-F(V/V_D)\cdot N_f\} \tag{12}$$

where $F(V/V_D)$ is the cumulative frequency of occurrence from Fig. 2, and N_f is the number of flights per life. Assuming a life of 50,000 flight hours, the F_{Va} functions obtained are shown in Fig. 3. The number of flights per 50,000 flight hours and parameters μ and β for each airplane are shown in Table 1.

It can be seen that the current practice of limiting the airspeed at V_C level provides a large margin of safety for the airspeed.

From the available statistics in the most scattered case of the CRJ100 aircraft, the probability of exceeding V_D is about 4.10^{-9} per life. According to [30], this might happen because the "aircraft's onboard computers should only allow these speed limits to be exceeded for a few seconds before automatically responding by reducing the aircraft's speed to acceptable levels." So calibration of the autopilot to not exceeding V_{MO} (airspeed limit as defined in the aircraft flight manual), which is close to V_C, leads to another informal safety measure against aeroelastic instability. In general, with automated control systems, the airspeed limit may then be established quite close to V_D.

For the following estimates of the POF, we use the conservative assumption that V_D may be attained one time per life ($\mu = 1$) and assume a CRJ100 shape parameter $\beta = 0.0063$. Then the equation

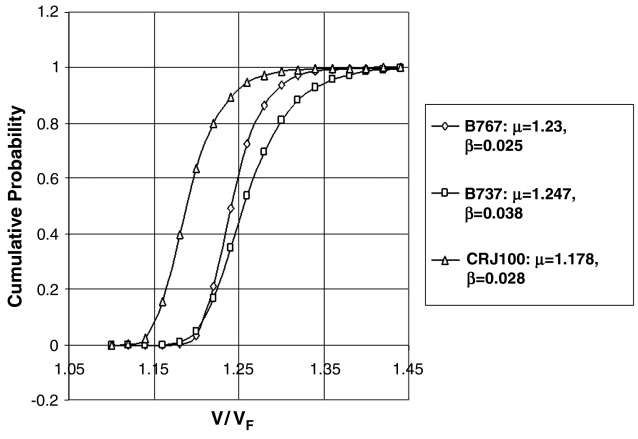

Fig. 4 CDF of maximum airspeed per 50,000 flight hours in flaps-extended configuration.

for maximum airspeed per the life of passenger airplanes is given as follows:

$$F_{Va}(V/V_D) = F_{Va}(z) = \exp\left[-\exp\left(-\frac{z-1}{0.0063}\right)\right] \quad (13)$$

References [28–32] also contain data on the probability of exceeding various airspeeds in flaps-down configurations. The operational airspeed limit (cockpit placard speed) has been used to scale the indicated airspeed. If this speed is equal to the design flap speed, it may be concluded that the safety margin for this configuration is much less than for the retracted flaps case. Assuming that V_F is analogous to V_C and, therefore, the flap-down configuration should be designed for $1.25 \times$ design flap speed, we can obtain the equation for F_{Va} (Fig. 4):

$$F_{Va}(V/V_{DF}) = F_{Va}(z) = \exp\left[-\exp\left(-\frac{z-1}{0.038}\right)\right] \quad (14)$$

With statistics of how airplanes are actually flown, in regard to their maximum speeds during their service life, we proceed to focus attention on the variability of airplanes in a fleet.

C. Probabilistic Characterization of Airplane Flutter Speeds in a Fleet

1. General

Acar et al. [33] provide a classification of different sources of uncertainty, which can be adopted for the present study. They propose a classification that distinguishes between 1) uncertainties that apply equally to the entire fleet of an aircraft model and 2) uncertainties that vary for the individual aircraft.

Type 1 uncertainties result from the uncertainties of particular aircraft model design and are fixed for a given aircraft model. Type 2 uncertainties are random and can be modeled probabilistically. Using different terms, the failure uncertainty may be divided into two types. To quote [33]:

> ...systemic errors and variability where systemic errors reflect inaccurate modeling of physical phenomena, errors in structural analysis, errors in load calculations, or use of materials and tooling in construction that are different from those specified by the designer. Systemic errors affect all of the copies of the structural components made and are therefore fleet-level uncertainties. They can reflect differences in analysis, manufacturing, and operation of the aircraft from an ideal. The other type of uncertainty reflects variability in material properties, geometry, or loading between different copies of the same structure and is called here individual uncertainty.

Following this classification, we may introduce three statistical variables. The first is $X = Vij/Vj$, Vij being the flutter speed of any one member in the jth fleet of nominally identical structures, while Vj is the mean flutter speed of the jth fleet. This variable X characterizes the type 2 (individual) uncertainties.

Each aircraft model is designed with systemic uncertainties. Suppose we can measure individual flutter speed V_f for all members of the jth fleet and get the mean value Vj. We can compare this Vj to the design flutter speed (DFS) $V_{\text{DFS}} = 1.15 \times V_D$.

Suppose now that Vj for all models designed under the same rules (say FAA rules) can be obtained. Then the accuracy of flutter speed prediction (type 1 systemic uncertainties) can be studied by using the variable $Y = Vj/Vj_{\text{DFS}}$. The third variable $Z = XY$ is used to study the uncertainty of flutter speed V_f for a whole population (all members of all fleets) with respect to the DFS. This population represents aircraft designed and manufactured using the same rules and procedures (e.g., FAA regulations), and the CDF $F_Z(Z)$ is a probability measure characterizing the flutter speeds of the population. With enough information, the $1.15V_D$ rule, which is valid for all fleets, is to be examined and evaluated from the reliability point of view, and the variable Z should be used for evaluation of the POF.

2. Uncertainties in Flutter Speeds of Individual Members of a Fleet

First, let us consider the variable X, which characterizes the scatter of individual flutter speeds in some fleet that has been designed with average Y ($Y = Vj/Vj_{\text{DFS}}$). The scatter of a critical flutter speeds among various members of a fleet results from the scatter in critical flutter-speed-determining parameters. We focus here on structural characteristics that affect linear flutter speeds, and most of these parameters can be considered as random variables. For a beamlike high-aspect-ratio wing structure, for example, this dependency can be expressed as

$$V_f = f[EI(y), GJ(y), m(y), I_m(y), x_{c.g.}(y), c(y), \ldots] \quad (15)$$

where EI and GJ are bending and torsion stiffness, respectively; the variables m and I_m are per unit span mass and moment of inertia of a wing; $x_{c.g.}$ is a position of the cross-sectional center of mass; c is the location of control surface and flap centers of mass, etc. Each of the structural parameters upon which the flutter speed depends exhibits certain scatter and can be treated as a random variable. The determining parameters are actually random fields, with spatial statistical variation, but for the discussion here, in the case of beamlike wings modeled using equivalent beam models (or any wings modeled using FEs), the wing can be divided into regions (panels and spanwise sections) with the properties of each region considered random parameters that are independent of neighboring section scatter. Spatial variability of structural properties within each region is allowed, as will be shown later when results of the prototype tail/rudder system used here will be presented.

Different parameters have different statistical characteristics. Some parameters exhibit wide scatters and need to have representative statistical description. Some parameters having relatively small scatter may be considered as deterministic or quasi deterministic. Thus, for example, for the studies presented here, which focus on linear flutter, the geometrical dimensions of aircraft are modeled as deterministic parameters. Note, however, that statistical variability of shape parameters becomes important in the structural case when local buckling of thin-walled elements is considered (the effect of initial imperfections) or in the nonlinear transonic flutter case, where airfoil and wing geometry variations can theoretically affect shock wave location and nonlinear unsteady aerodynamics and flutter speeds.

In the discussion here, the functional dependence of flutter speed on structural parameters in Eq. (15) is determined by special analyses and tests, with Eq. (15) representing a deterministic function of uncertain parameters.

Generally, this relationship is rather complicated; hence, the effects of variation in determining parameters on the resultant flutter speed are complex. However, statistical sensitivity analysis can usually identify those parameters that have the strongest influence on particular critical speeds, such as flutter, divergence, and aileron reversal speeds. Therefore, the scatter of critical speed for various fleet members will be, first of all, connected to the dispersion of those influential parameters.

For the domain of existence of the flutter speed function $V_f(x_1, x_2, \ldots, x_n)$, the problem of determination of the PDF of the random variable V_f can be formulated as follows. Assuming that there exists a deterministic function of several random arguments $V_f(x_1, x_2, \ldots, x_n)$ and that the arguments x_i have a known joint CDF $F_x(x_1, x_2, \ldots, x_n)$, the CDF of V_f is then determined from probability distributions of the system random variables $x_1, x_2, \ldots, x_n$:

$$F_{Vf}(y) = \iiint_{\Omega Y} \ldots \mathrm{d}F_x(x_1, x_2, \ldots, x_n)$$

$$\Omega_Y = \{(x_1, x_2, \ldots, x_n)\colon V_f(x_1, x_2, \ldots, x_n) \le y\} \quad (16)$$

If the variables x_i are statistically independent, then

$$\mathrm{d}F_x(x_2, x_2, \ldots, x_n) = \mathrm{d}F_1\,\mathrm{d}F_2 \cdots \mathrm{d}F_n \quad (17)$$

Considering the complexity of $V_f(x_1, x_2, \ldots, x_n)$, we can expect that the PDF of V_f will also be rather complicated. For approximate estimations of the POF due to aeroelastic mechanisms, a linearization of this function is often used in the vicinity of some characteristic average point $x_1, x_2, \ldots, x_n$:

$$V_f(x_2, x_2, \ldots, x_n) = V_f(\bar{x}_2, \bar{x}_2, \ldots, \bar{x}_n) + \sum_{i=1}^{n} \frac{\mathrm{d}V_f}{\mathrm{d}x_i}(x_i - \bar{x}_i) \quad (18)$$

Such an approximation can yield accurate results when the variances σ_{xi}^2 of random arguments x_i are small. For many problems of practical importance in aircraft structures, the relative scatter of the determining parameters is, indeed, rather small, and the statistical description of a function $V_f(x_1, x_2, \ldots, x_n)$ by means of Eq. (18) can be quite appropriate. In such cases, if the x_i are statistically independent, the parameters of PDF for V_f can be determined from

$$\bar{V}_f = V_f(\bar{x}_2, \bar{x}_2, \ldots, \bar{x}_n); \qquad D_{Vf} = \sigma_{Vf}^2 = \sum_{i=1}^{n} \left(\frac{\partial V_f}{\partial x_i}\right)^2 \sigma_{x_i}^2 \quad (19)$$

But care must be taken here. As will be shown later in the paper, there can be cases where small variations of fundamental parameters, due to flutter mechanism switching, can lead to discontinuous flutter speed derivatives. The need in such cases is to capture the statistics of the resulting flutter speed by Monte Carlo simulations or higher-order methods than Eq. (18) for approximating the nonlinear dependency of flutter speeds on the parameters affecting it.

Now, as has already been mentioned, experimental data on the scatter of natural frequencies of full-scale aircraft structures are given in [25]. The modal tests of three nominally identical large commercial airplanes built mainly of aluminum alloys had shown that the coefficient of variance (COV) of the natural frequency of the main modes (bending of wing, tail unit, fuselage and pylons, and torsion modes of various structural parts) lay within the limits of COV $C_V = 0.012$ to 0.03 (mean value for all modes is 0.021). The modal tests of five metal passenger airplanes yielded the C_V of the main structure natural frequency between 0.013 and 0.072 (mean value is 0.04).

The data on stiffness parameters for composites available in MIL-HDBK-17 [34] show that their scatter is at least twice as great as the typical scatter for aluminum alloys. Flutter speed analyses of the example composite vertical tail/rudder system, considered later in this paper, showed that the resulting COV of flutter speed for a composite structure was about 9%, which is more than two times greater than that for metal due to variations of the material properties.

Regarding the shape of the probability distribution of flutter speeds, statistical data in the literature are scarce. A previous study [24] in which the shape of flutter speed PDF had been obtained for a three-degree-of-freedom aeroelastic system using Monte Carlo simulations, showed that the flutter speed distribution was approximately normal. Seventeen structural input random parameters were considered in a rather realistic manner in that study. Another probabilistic study of a realistic vertical tail/rudder system, which will be presented toward the end of this paper, shows that the shape of the V_f distribution may be much more complicated than the normal PDF.

But since the main goal of this section is to present a probabilistic methodology for the flutter failure assessment of aircraft, including the effect of flight tests, normal PDF and plots in normal PDF scale will be used first. The methodology is general, however, and can address cases in which probability distribution functions of flutter speeds in a fleet are not normal.

So a conditional normal distribution $f_X(X) = f_X(X|Y)$ is used first for the probabilistic description of the variable X, characterizing the individual uncertainties of the flutter speed. The mean value of this PDF is Y, which is uncertain itself, because it is obtained by analysis with all the systemic inaccuracies inherent in a selected analytical method. The COVs are taken, for the sake of the following discussion, to be known and equal to $C_V = 0.09$ for composite structures.

D. Systemic Uncertainties

The random variable Y defined earlier is going to be used for the characterization of the flutter design method with its systemic errors. By definition, $Y = \bar{V}_f/V_{\mathrm{DFS}} = V_j/V_{j\mathrm{DFS}}$ is a fleet average flutter speed for fleet j relative to its DFS. The PDF of this variable can be determined as follows.

Obviously, the statistical properties of Y reflect variations of flutter speed prediction/design accuracy across several fleets (one airplane model per fleet) using the same flutter analysis and design technology and may be obtained by the comparison of analytical flutter predictions with test results. Such comparisons in the open literature are usually provided by commercial software developers who want to demonstrate the accuracy of their codes. It is much more difficult to obtain analysis/test correlations from airplane manufacturers, and analysis/test correlations depend on more than just the FE and unsteady aerodynamics methods used. They depend also on modeling practices, modeling assumptions (especially regarding structural damping), etc. To present the methodology proposed here, the available data of [5] are used to generate an empirical distribution of the ratio-predicted flutter speed/measured flutter speed. The empirical CDF, usually called simply an empirical distribution function or empirical CDF, is a CDF that assigns probability $1/n$ to each of the n numbers in a sample. The empirical CDF, drawn in Fig. 5, for 12 cases shows that, on average, the data used reflect quite unconservative estimates of V_F. Proceeding with these data (but with a method that allows incorporation of any industrywide data that may be more realistic), let us assume that actual flutter speeds, on average, are $1/1.11 = 90\%$ of analytically predicted (design) flutter speeds, with an error of 9% standard deviation. As FAR 25 [1] states that the DFS should be not less than $1.15V_D$, the PDF $f_Y(Y)$ in the illustration here is conservatively assumed to be the normal distribution with the mean $= 0.9 \times 1.15V_D$ and $\sigma = 0.09$.

E. Flight Testing

In compliance with FAR 25.629 [1], full-scale tests must demonstrate that the airplane has a proper margin of damping at all speeds up to $V_{\mathrm{DF}}/M_{\mathrm{DF}}$ and that there is no large and rapid reduction in damping as $V_{\mathrm{DF}}/M_{\mathrm{DF}}$ is approached. The way to quantify that large and rapid reduction is an extrapolation of damping versus airspeed up to $1.15V_D/M_D$.

Let it be assumed that there is a world population of aircraft designed in compliance with FAA requirements and particular industry rules and practices, and with systemic errors of state-of-the-art analysis and design methods. This population incorporates N different aircraft models. They are designed with systemic errors specific to each model. The fleet of each model consists of M_J ($J = 1, \ldots, N$) members. It is desirable to obtain the PDF of the flutter speed for this world population of aircraft with known individual uncertainties characterized by the random variable X and systemic uncertainties characterized by the random variable Y. Both $f_X(X|Y)$ and $f_Y(Y)$ were defined earlier in the subsections where individual and systemic uncertainties were discussed. To simplify the considerations for the present exploratory study, it is assumed here that the flutter speed scatter in all fleets manufactured of similar materials and using similar technologies may be characterized by PDF with the same COV of the variable X, $C_{V_X} =$ constant. It is also

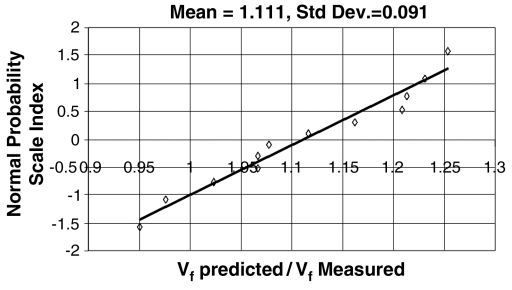

Fig. 5 An example of empirical CDF for the accuracy of analytical flutter prediction.

assumed that the predicted flutter speed for each fleet is the same as DFS (most conservative assumption reflecting, maybe, aeroelastic optimization design practices), and this speed is equal to $1.15V_D$.

The goal here is to show how flight tests of one aircraft in a fleet affect the mentioned population. First, the population will be numerically sampled assuming that there have been no flight tests. For the N model types, N random values of Y can be found and (for simplicity) for each of the models, the same number M of X random values (for each Y) will be sampled as follows:

1) A fleet (model) $Y_{J.}$ is randomly generated from the $f_Y(Y)$ distribution defined previously.

2) In this fleet, M individual flutter speeds $X_{i.}$ $(i = 1, \ldots, M)$ are randomly generated using the $f_X(X|Y)$ distribution with values of Y_j generated in step 1.

3) Steps 1–2 are repeated $N - 1$ times $(j = 1, \ldots, N)$.

4) The empirical CDF of flutter speeds in the fleet relative to respective design dive speeds are drawn, and the two first moments (the mean and C_V) are calculated.

The result is the world population without flight-test substantiation. It is named, here, prior population, and it is characterized by the prior CDF.

A posterior CDF characterizing the population as it is after flight tests can then be obtained using the following steps:

1) A fleet (model) $Y_{J.}$ is randomly generated using the $f_Y(Y)$ defined previously.

2) In this fleet, M flutter speeds X_{ij} are randomly generated for M aircraft using the $f_X(X|Y_j)$ with a value of $Y = Y_j$ generated in step 1.

3) One aircraft in this fleet is now randomly selected from the fleet with its corresponding X_i. This aircraft is tested in flight at V_D or a lower speed, and it is concluded that the normalized actual flutter speed is $X_{jm}. = V_{fm}/V_D/1.15 +$ random error of measurements (with extrapolation). The term $V_D \times 1.15$ is an analog of the design ultimate load when V_D is similar to the limit load in static strength design and is 1.15 analog of the safety factor. The flutter flight test is analogous of the static test for which the main function is to reduce systemic uncertainty. It should be mentioned here that the flight test itself is subject to errors that can affect flutter speed prediction [35–39].

4) If $X_{jm} < 1 (V_{fm} < V_D \times 1.15)$, all the aircraft of this fleet/model are redesigned so that their flutter speed is ideally increased by $1/X_{jm}$. If $X_{jm} > = 1$, our model/fleet is certified without redesign and goes to operations. Go to step 7.

5) When redesign is required, then in the redesigned fleet, one structure is randomly chosen with its respective X_{ij}.

6) Step 3 is now repeated to conduct another flight test. The process is terminated when a test shows acceptable flutter speed flight. The ratio of measured flutter speed to predicted flutter speed, reflecting systemic errors, can now be used, and the simulated statistical data for one fleet can be generated.

7) As we assumed that N fleets are available, the previous steps should be repeated N times to obtain $N \times M$ normalized flutter speeds X_{ij} for the whole aircraft population.

8) Now an empirical CDF for this population is drawn, and the two first moments are calculated (mean and $C_{V.}$) for the distribution of flutter speeds (relative to respective V_D design requirements) in a fleet, given the results of flutter flight tests and any design changes met to meet certification criteria.

Note that decisions about whether an airplane meets flutter requirements or not can also based on flight flutter test results showing freedom from flutter up to VD with sufficient damping at VD and no rapid decay of damping up to $1.15VD$. We use the requirement of freedom from flutter up to $1.15VD$ here and focus on the tests producing an experimental flutter speed value.

The scheme described previously was implemented using Monte Carlo simulations, and the results of those simulations are shown in Fig. 6, where the empirical CDFs before flutter flight tests (prior) and after flutter flight tests (posterior) are shown. One hundred aircraft models were simulated with 100 aircraft per fleet. The values of prior CDF mean and COV used for random number generation were 0.9 and 0.09, respectively. The mean and COV shown in Fig. 6 were obtained from the generated sample. That is why they are a little bit different from 0.9 and 0.09. The same stands for all subsequent related figures.

The flight tests are obviously contributing to shift the CDF to the right (increased safety). The greater slope of CDF curve means the reduced scatter and, therefore, the increased safety. It should be mentioned here that only a 1% flight test error and extrapolation uncertainty was included in step 3 for the example presented here. A more realistic value of that error [35–39] may reduce the slope of the appropriate CDF curve with a corresponding reduction in safety.

Now let us assume that designers know about systemic (analytical) errors and therefore designed all the fleets conservatively with an initial flutter margin of 1.22 in addition to the required margin of 1.15. This means that the average value of the normalized variable Y is now $0.9 \times 1.22 \approx 1.1$. Figure 7 shows the CDF function of the normalized flutter speed distribution in a fleet when models are initially designed with a 22% redundancy to compensate for the systemic errors discussed previously.

F. Contribution of Other Safety Measures

In compliance with Sec. 5.3 of [40] some factors may be applied that lead to design values that are lower than base material properties, including the stiffness requirements (flutter or vibration margins). As the data on stiffness parameter scatter for composites are available in MIL-HDBK-17, proper design values similar to the A/B basis used for failure stress may be derived. The derivation of an A-basis value for typical data on composite elastic moduli described by the Weibull PDF with COV = 8% leads to a stiffness reduction factor of 0.77. The parametric analysis of the composite vertical tail/rudder system described later in this paper shows that such a factor results in a flutter speed margin of about 15% above the usual factor of 1.15 in that case. This value of the additional flutter speed margin for composite structures is used in the present study for the evaluation of the POF, presented next.

G. Probability of Failure

The considerations, assumptions, and statistics discussed previously can now be applied to the evaluation of the POF due to flutter. At this point in the study, it is first assumed that there is no significant

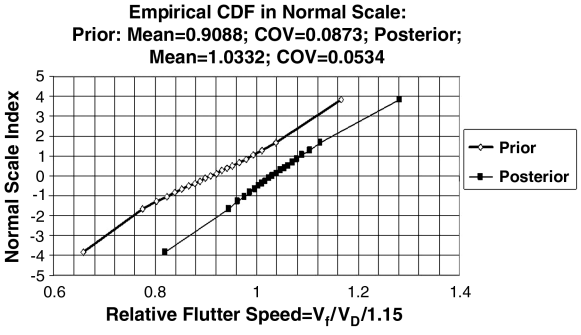

Fig. 6 CDF of flutter speed before and after flight tests: unconservative design with no damage assumed.

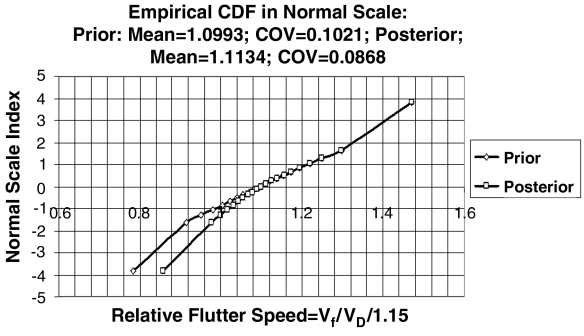

Fig. 7 CDF of flutter speed before and after flight tests (systemic analysis errors accounted for): conservative design with no damage.

Table 2 Probability of flutter failure of metal and composite structures[a]

	Analysis only				Analysis supported by flight tests			
	Mean Y	C_V, %	POF, flaps retracted	POF, flaps extended	Mean Y	C_V, %	POF, flaps retracted	POF, flaps extended
Metal structure: model mean COV = 9%, *fleet articles* COV = 4%, *and test extrapolation* $C_V = 1\%$								
Unconservative design	0.9	8.7	0.33	0.45	1.033	5.3	9.9E − 4	0.025
Conservative design	1.099	10.	0.012	0.031	1.113	8.7	4.4E − 4	0.007
Composite structure: model mean COV = 9%, *fleet articles* $C_V = 6\%$, *and test extrapolation* $C_V = 1\%$								
Unconservative design	0.9	10	0.44	0.45	1.042	8.1	0.017	0.05
A allowable for stiffness	1.15	12	0.01	0.03	1.16	10	0.0026	0.013
Design for 1.25 flutter factor, mean $Y \sim 1.25V_D$	0.9	9	0.1	0.22	1.03	5	3.81E − 6	0.0078

[a]For the POF results shown here, we use the conservative assumption that V_D may be attained one time per life. In fact, according to Fig. 3, only $0.86V_D$ is attained one time per life.

time-dependent structural degradation per structural life. That is, there is no material degradation with time and no damages are accounted for first. The posterior X_{ij} simulation results of Fig. 6 can thus be used.

Since the failure event is defined here as flight airspeed exceeding the X_{ij}, and the probability that airspeed does not exceed X_{ij} is described by Gumbel CDF, the probability of exceeding the X_{ij} for individual aircraft in the population is

$$P_{Fi} = 1 - \exp\left[-\exp\left(-\frac{1.15 \times X_{ij} - \mu}{\beta}\right)\right] \tag{20}$$

From Eq. (13), $\mu = 1$ and $\beta = 0.0063$ for the flaps-up configuration. The average of this random value over the entire population would be the integral measure of safety against flutter.

It would be consistent to also consider the flaps-down flight segment. The maximum speeds for the flaps-down configuration are described by Eq. (14) with parameters $\mu = 1$ and $\beta = 0.039$. In general, the available flutter speed margin may be greater than 15%, but we assume here that the aircraft structures in all fleets are perfectly optimized for this factor plus an additional factor of 1.15 for the elevated stiffness scatter of composite materials.

Table 2 shows the probability of flutter failure of metallic and composite aircraft calculated based on analysis only and on analysis corrected by flight-test results. It also shows the effect on the probability of flutter failure of using nominal and reduced material stiffness data. Instead of the reduced material stiffness data, this probability may be reduced by specifying the elevated flutter speed margin for composite structures. The POF for a margin of 25% instead of 15% is calculated and presented in Table 2.

Considering the data of Table 1, it may be concluded that the flutter flight test is a very efficient safety measure that reduces the uncertainty in analytical models and, eventually, it helps to shrink the scatter of flutter speeds in a global aircraft population. In the most important cases, if a flutter flight test is conducted, this leads to a significant reduction of the POF. A note should be added here regarding the contribution of wind-tunnel flutter tests to the assessment of systemic analysis errors. This can also be addressed as part of the numerical modeling effort leading to the design, and then the flight flutter test.

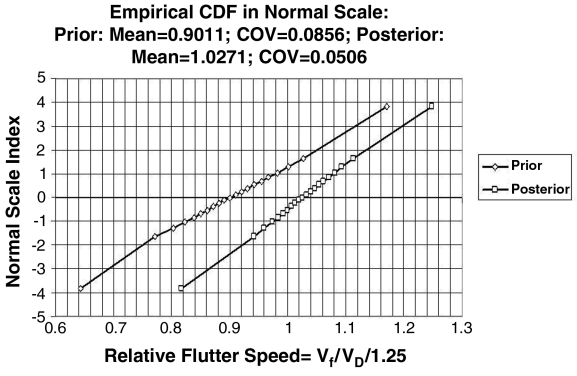

Fig. 8 CDF of flutter speed with a margin of 1.25: unconservative design.

A combination of unconservative design with flight tests provides the minimum dispersion of flutter speed at minimum extra weight.

Introduction of a reduced stiffness A-basis allowable is rather efficient but not a sufficient safety measure. The more adequate safety measure seems to be, based on the example here, increasing the aeroelastic stability margin for composite structures up to 25%. The empirical CDF for this case is shown in Fig. 8. It is emphasized that this conclusion is limited to the studies based on the assumptions presented here and that more complete and realistic data may lead (using the present methodology) to different conclusions.

The posterior CDF shown here will be used for POF calculations for a composite structure subject to possible damage. We now shift focus from the case of pristine structures that do not change with time to the case of airframes that change over time due to material degradation and possible damages.

IV. Probability of Flutter Failure with Changes of Airframe Dynamic Properties over Time

A. General

All estimates of probability of flutter failure, obtained previously using the methodology presented here, were based on the assumption that the structural properties contributing to aeroelastic stability were unchanged over the airplane time of operation. This assumption is supported by modal tests of aircraft in operation and modal tests conducted during fatigue testing in the laboratory. The most important changing parameters mentioned in publications on metal structures [25] are structural damping, dry friction, and certain parameters of the control system. Structural damping can usually increase $1.2, \ldots, 1.3$ times per life due to the loosening of joints. Increased free play of control surfaces due to joint wear has been identified as a cause of limit cycle oscillation (LCO). The dynamic properties of control surfaces, high-lift devices, landing gear, and other similar actuated structural components vary noticeably with time during operations because of the general loosening of joints between parts, the rough repair of lightweight honeycomb structures, the wear in hinges, etc.

As composite materials are becoming more widely used in primary structures, three major concerns have been raised in the literature: 1) stiffness degradation due to impact damage (localized or spread), 2) material aging and mass property changes due to environmental exposure and water absorption, and 3) mass property and stiffness changes due to repair. These may be rather substantial, especially for control surfaces. In the following, an evaluation will be presented of the impact of such typical features of composite airframes on flutter characteristics using a model of a representative composite vertical tail/rudder system. Since the problem is quite similar to the problem of residual strength, the POF assessment method proposed by Lin and Styuart [3] will be used.

B. Addressing Material Degradation, Environmental Effects, Inspection Procedures, Damage, and Repair

In a way similar to the approach used in damage tolerance, an airframe that sustained damage or has seen material degradation will

have a residual flutter speed that may be lower than its original flutter speed. The assessment of the POF for residual flutter speed history (accounting for damage and repair during the lifetime of the system) is shown schematically in Fig. 9. As the figure shows, damage to the structure and subsequent repairs may lead to changes in local stiffness and mass and to changes in linear flutter speed. Damage statistics covering damage size, damage type, damage time of appearance, and duration before repair (depending on maintenance procedures) are converted to a history of residual flutter speed variations. Combined with statistics of flight speeds attained by aircraft in service, it is now possible to assess the probability that some flight speed attained might reach the flutter speed of a damaged or repaired structure. Thus, the POF due to flutter can now be evaluated.

As an example, let us assume that some structural component or system has the following residual flutter speed history: initial flutter speed of the new system equaling $1.15V_D$. Then, at the instant $t_0 = 0.4$, impact damage occurs (due to hailstorm, for example), and the flutter speed is decreased to the value of $1.075V_D$. As some impact damages may be almost invisible, this damage is not detected until the time instant $t_1 = 0.6$ when the damage is repaired, but the flutter speed is restored only partially to a value of $1.1V_D$ due to changes of mass properties (e.g., honeycomb trailing edge). There are three intervals t_i here of constant flutter speed for the system, and failure may happen because of the occurrence of flight air speed that exceeds the critical residual flutter speed sometime during the life of the vehicle. Simple calculations are included in Fig. 9. The final POF is equal to one minus the product of the POFs, and it does not happen

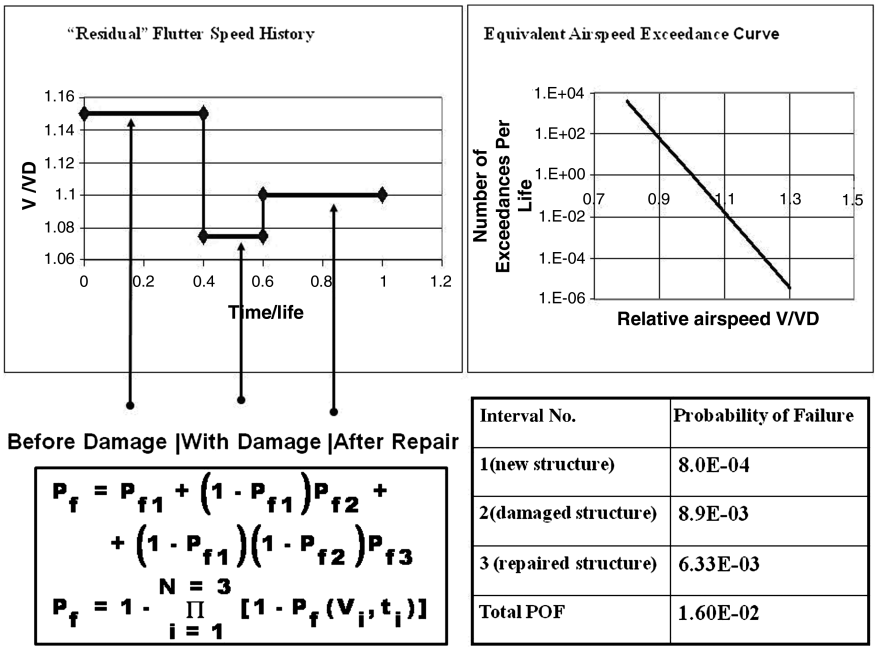

Interval No.	Probability of Failure
1(new structure)	8.0E-04
2(damaged structure)	8.9E-03
3 (repaired structure)	6.33E-03
Total POF	1.60E-02

Fig. 9 POF accounting for the possibility of damage and repair: formulation 1.

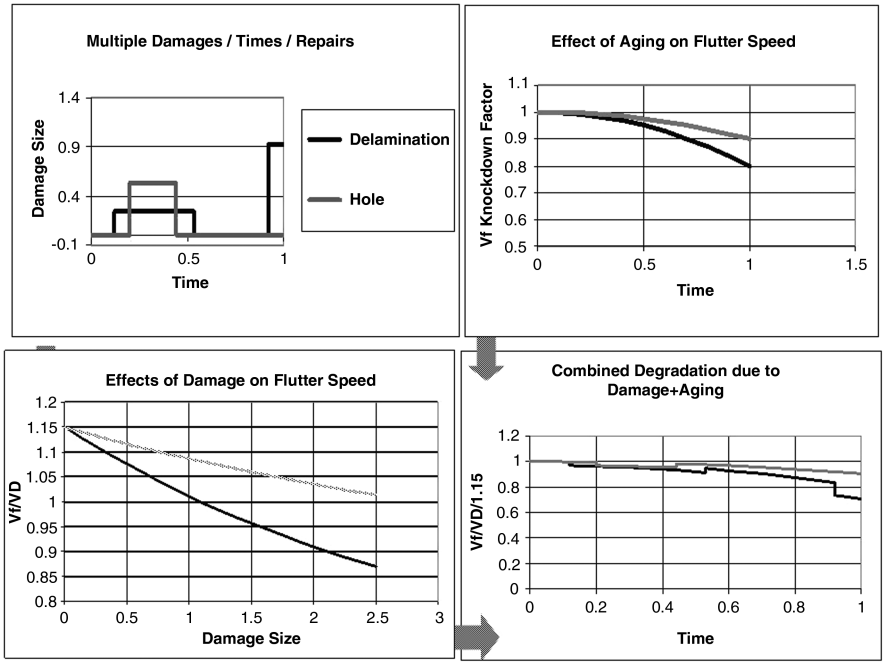

Fig. 10 A second approach to probability of flutter failure showing effects of delamination (solid black line), holes (gray), material degradation, and repair.

in each of the three intervals. In calculating the POF in each of the time intervals, an account is taken of flight speed statistics, residual flutter speed, and the duration of the interval.

A more realistic case is considered next, in which the number of damages per life may be more than one; there may be several different types of damage (e.g., through crack, indentation, delamination, disbonding, etc.) as damages occur at random times and have different random sizes. There may also be several different types of inspection methods used (preflight visual inspection, maintenance inspection using different techniques, etc.). The time of damage existence (damage life) depends on the frequency of inspections and the capability of inspection to detect damage. Finally, the aeroelastic properties may also change because of material aging, water absorption, etc.

Figure 10 shows one history of random damage size vs time, simulated using the Monte Carlo method. Two types of damage are considered: delamination and hole. The damage size realization can be converted (via residual stiffness assessment) into residual flutter speed realization, and the POF then calculated is similar to one shown in Fig. 9.

The POF is assessed based on simulation of random histories of damage size and time throughout the life of a structure. Each history consists of a number of constant damage size intervals. The starting time of each interval is a random value, and the length is a random function of the probability of damage detection (depending on detection methods used and the training of inspection professionals) and inspection frequency. Histories may be randomly simulated using a finite set of primitive random variables such as damage occurrence rate and probability of damage detection. The damage size may be converted into the appropriate random residual stiffness and then to residual flutter speed, where the reduction of the stiffness occurs due to the presence of both manufacturing defects and accidental operational damage. In addition to stiffness, mass properties may be changed as a result of repair.

The Monte Carlo damage generation module described earlier varies primitive random variables: the number, type, and size of the damage and defects; the time of damage initiation; the number of inspections to detect damage; the initial and residual stiffness as a function of damage size; stiffness/mass after repair; and maximum airspeed within constant damage size interval. Temperatures and temperature/humidity effects can be added as well. Using the automated flutter simulation tools described at the beginning of the paper, the resulting flutter speeds are determined and used to evaluate the POF.

Current models and simulation capabilities developed at the University of Washington are capable of handling any number of defects/damages (upper limit is specified by user), various types of damages, inspections and monitoring, nonuniform inspection schedules, and various maintenance decisions for detected damage repair.

V. Exploratory Studies: Uncertain Aeroelastic Composite Vertical Tail/Rudder System

A. Structure

A realistic NASTRAN model of a composite vertical tail/rudder system of a passenger airplane (but not representing any actual flying vehicle) is presented in Fig. 11. Generally, flutter analysis and certification of tail surfaces is carried out for the coupled tail/empennage or tail/aircraft system to account for the effect of fuselage motion and root conditions on the flutter speed, but for the exploratory study presented here, the nodes at the root ends of the spars were fixed.

The tail structure is assembled from several separately manufactured panels. Thus, panel-to-panel variability should be considered. Properties of structural subcomponents manufactured separately, are assumed independent. As each panel is divided into FEs, the element-to-element variability should be accounted for as well. The properties of individual FEs belonging to skin panels, spars, stringers, and frames are considered correlated within each panel, spar, etc. Obviously, the properties of the neighboring

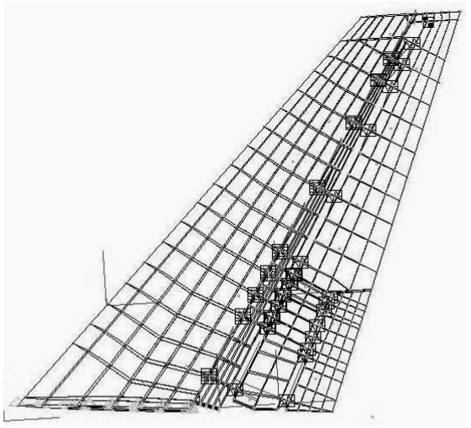

Fig. 11 Representative composite vertical tail/rudder finite element model.

elements are closely correlated, and this should be properly considered. Some probabilistic aeroelastic studies to date involve simple aeroelastic models, such as beamlike wings with the spatially distributed uncertainties considered in a form of Markov field. The covariance kernel of the random field is often assumed in the form,

$$C(x, x_1) = \sigma_p^2 e^{(-|x-x_1|)/R_{\text{cor}}} \tag{21}$$

where σ_p^2 is a field variance and R_{cor} is a radius of correlation. This model is used in the current study. The model random input is characterized by the variability data shown in Table 2 (PSHELL element properties). The typical COV values of the Table 2 parameters were taken from MIL-HDBK-17. Theoretically, the radius of correlation could also have been evaluated from the data of the MIL-HDBK-17 if the appropriate supporting information like panel size and coupon size were present there. The COV of thickness and Young's modulus for PBAR and PROD properties were assumed equal to 0.02. The same value has been used for CONM2 mass elements. The NASTRAN model of the system was modified to allow every structural and mass element to have its own property and material card. The elements belonging to structural panels that are manufactured separately were united into groups to represent panel-to-panel variability (Table 3).

Attention was paid to adequate simulation of the composite skin panels where impact damages were expected. Those structural panels were simulated using NASTRAN SHELL FEs with randomized thickness and three random material properties: $G11$, $G12$, and $G22$. Since the example FE model (Table 4) arrived with lumped masses representing mass distribution for dynamics purposes, the material density was simulated as included in those lump masses. The correlation between the local thickness and structural mass of each FE was not simulated due to the lack of appropriate information for this particular model. Average panel geometric and materials properties were simulated independently, while those of individual FEs belonging to each panel were simulated using the Markov random field.

B. Unsteady Aerodynamics

Figure 12 shows the aerodynamic model used for the vertical tail/rudder system. The unsteady aerodynamics is based on the doublet

Table 3 Variability data for the composite tail/rudder system (PSHELL element properties)

Property	Panel-to-panel COV	Element-to-element COV	Radius of correlation, in.
Thickness t	0.03	0.01	10
$G11$	0.05	0.02	100
$G22$	0.05	0.02	100
$G12$	0.05	0.02	100

Table 4 The NASTRAN FE model of the composite tail/rudder system

Element	Amount
Grid points	1268
CBAR	309
CBUSH	45
CONM2	28
CQUAD4	1409
CROD	1056
CSHEAR	91
CTRIA3	187
RBE2	16
RBE3	28

lattice method (although, as stated earlier, ZAERO has also been used in our automated flutter simulation capability). The aerodynamic reference surface on the plane x-z is divided into five trapezoidal macropanels. Each macropanel is subdivided into strips of trapezoidal panels. Surface splining for information transmission between structural and aerodynamic points is taken care of by NASTRAN. It should be noted that, in this model, the trapezoidal surfaces 1, 2, and 3 have the same number of aerodynamic elements in the wingspan direction. Similarly, surfaces 4 and 5 have the same number of aerodynamic elements in the wingspan direction. The root of the structural FE model of the vertical tail was not exactly parallel to the axis of the incoming flow. The aerodynamic reference surface was slightly adjusted to direct the root in the x direction.

C. Free Vibration

Figures 13 and 14 show, for illustration, the free vibration mode shapes of the nominal structure with natural frequencies close to a flutter frequency of about 13 Hz. The automated flutter simulation capability efficiently produces mode shapes and natural frequencies for any variation of the aeroelastic system analyzed. Carrying out structural dynamic and flutter simulations of large numbers of variants of the aeroelastic system analyzed is what we name virtual tests. Actual natural modes contributing to the flutter mechanism vary, depending on variations in the structure and possible switching of flutter mechanisms, depending on the magnitude and combination of structural changes.

D. Virtual Flutter Test Results

The most interesting results of the virtual flutter tests are shown in Figs. 15 and 16. Figure 15 shows the empirical CDF of the flutter velocity. It is obvious that the corresponding PDF is bimodal. This

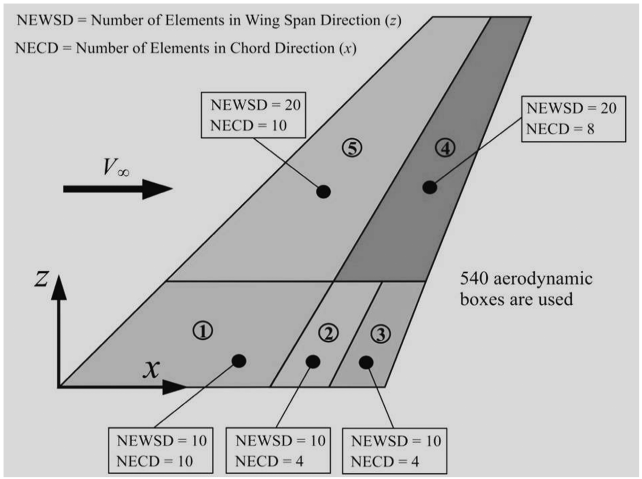

Fig. 12 Vertical tail/rudder system: aerodynamic model (doublet lattice method) showing the number of spanwise and chordwise aerodynamic box divisions for each large panel.

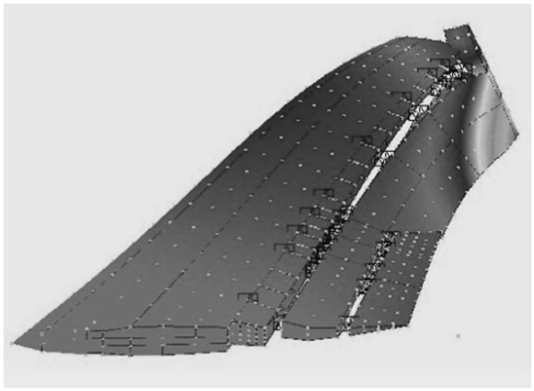

Fig. 13 Free vibration mode shape of the nominal structure, frequency = 16.34 Hz.

fact is reflected in Fig. 16, where the corresponding histogram is shown. Practically, this means that some aircraft in a fleet, simulated using the assumptions listed previously, may have flutter mechanisms rather different from the main population. It is also evident that the variance of the second flutter mechanism is much smaller than the first one. This may be evidence of different uncertainty propagation for different failure modes. In this particular case, the second mode of PDF is on the right steep branch of cumulative distribution function, which does not contribute much to the POF. But there may be situations when this mode may appear on the left tail. It is also obvious that some popular fast reliability methods, like the first-order and second-order reliability methods [41], may not be generally applicable to the probabilistic study of flutter and similar aeroelastic phenomena.

Another observation is that the variance of V_F is noticeably greater than variances for input parameters, shown in Table 3. This is not a general conclusion and seems to be case dependent, since earlier

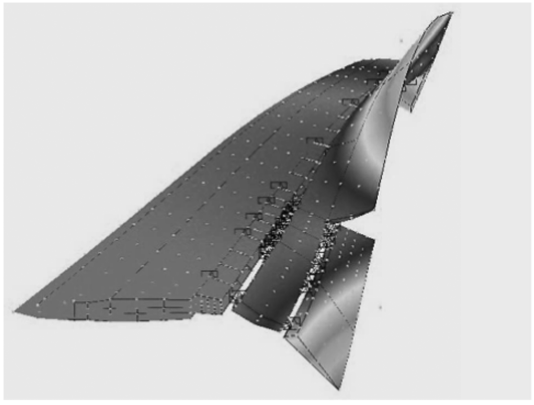

Fig. 14 Free vibration mode shape of the nominal structure; frequency = 18.24 Hz.

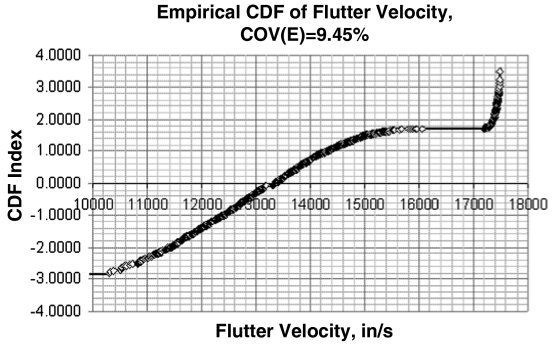

Fig. 15 CDF for vertical tail flutter velocity (no damage).

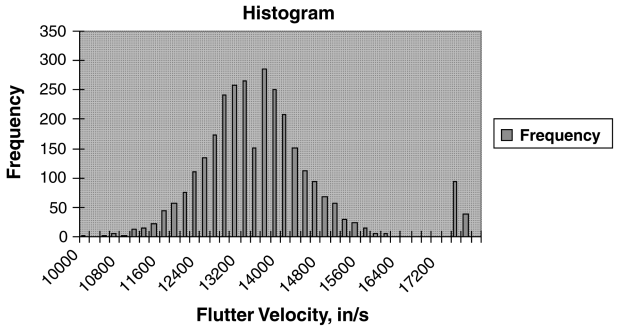

Fig. 16 Flutter velocity histogram (no damage).

studies using a simple delta wing model led to different distribution characteristics. The results here, then, serve to demonstrate the methodology and capability of the probabilistic flutter reliability assessment system presented, and they do not serve to draw any general conclusions regarding the reliability of particular aeroelastic systems types.

E. Virtual Flutter Tests of a Damaged Structure

Figure 17 shows the empirical CDF of the flutter speed V_F obtained with our VATM under the condition that a randomly selected element belonging to the tail torsion box skin has large damage of the size of about 150 mm.

Only stiffness reduction due to damage was considered and estimated (by using analysis of the element itself) as the difference of average relative displacements of opposite nodes per given loading depending on damage size. The damage was assumed at a center of the element. The locations of damaged elements have been chosen randomly, with uniform distribution over the tail box skin area.

As in [3], for the exploratory studies presented here, the residual panel stiffness has been determined using expressions based upon a rule of mixtures for a constant thickness panel:

$$\kappa_T = \left(\frac{W - W_D}{W}\right)\kappa_{T(U)} + \left(\frac{W_D}{W}\right)\kappa_{T(D)}$$
$$\kappa_C = \left(\frac{W - W_D}{W}\right)\kappa_{C(U)} + \left(\frac{W_D}{W}\right)\kappa_{C(D)} \tag{22}$$

where W is the total cross-section width of an element; $W = 250$–450 mm; W_D is the maximum cross section of damage size normal to the direction of the applied load (in the case of hole and delamination, damage is modeled here as circular in shape); $\kappa_{T(U)}$ is the original tensile stiffness of the composite; $\kappa_{T(D)}$ is the tensile stiffness of the damage region, which is negligible for hole; $\kappa_{C(U)}$ is the original compressive stiffness of the composite; and $\kappa_{C(D)}$ is the compressive stiffness of the damage region, which is negligible for hole.

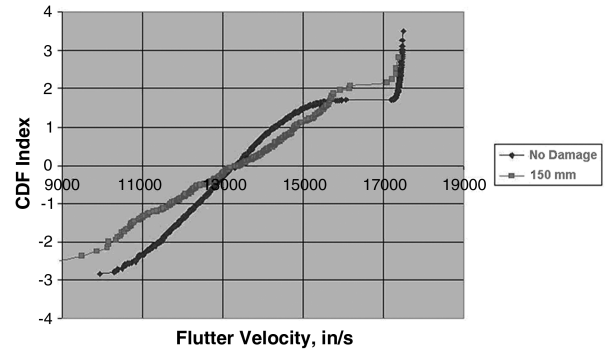

Fig. 17 Empirical CDF of V_F for the damaged and undamaged structures.

The cross-section width of an element has been defined for each randomly selected element in the direction coinciding with an aircraft longitudinal axis at the position of the element centroid.

The V_f CDF for the undamaged structure is shown in Fig. 17 for comparison. It is interesting to note that the average values are almost the same, but the COV of the damaged structure is much greater. This behavior is rather different from the results of previous studies using a simple delta wing model [42], where the average decreased with the damage size but the COV remained nearly constant. Both behaviors will inevitably lead to lower reliability.

F. Flutter Reliability of Damaged and Undamaged Composite Airframes

We finally use the methodology and capabilities described here to compare flutter failure reliability of undamaged and damaged composite airframes in the particular case of the tail/rudder example presented previously. Input data for the University of Washington's reliability life-cycle analysis of composite structures [3] were taken from [43–46]. Panel weight change due to repair was not considered due to the lumped mass nature of both structural and nonstructural mass in the model provided for this work by the industry. The V_f CDF for undamaged structure and damaged structure were taken by polynomial approximation of curves shown in Fig. 17 and other curves obtained with our virtual aeroelastic testing capability for different damage sizes.

The following input data were used: 1) number of design cases = 1 (subsonic flight); 2) number of damage types = 2 (hole and delamination); 3) number of inspection types = 2 (visual and Instrumental); 4) the CDF of maximum airspeed per life is expressed by Eq. (13) [see also Eq. 3 in [45] and the discussion there]; and 5) the probability of the damage detection model described in [3] was used.

The exceedance data of damage occurrence are taken from [47] and recalculated for 60,000 flight hours and the torsion box skin area. To introduce even more conservatism, the damage sizes in the calculations were twice as large as those in [47]. This might include the damages inflicted by uncontained turbine blades and similar cases.

Figure 18 shows the POF in flutter accounting for damage depending on the safety margins used for design. The POF without damages as a function of the safety margin used for design is also shown for comparison.

It should be mentioned that the representative vertical tail/rudder system here has about a 57% safety margin above V_D by design, and it is highly safe. The probabilistic analysis in the example presented here shows that, in order to ensure the same POF (as in the no-damage case), the safety margin with nominal stiffness should be at least 5% greater than that without damage considerations. This conclusion, it should be emphasized, is not general and is case dependent. Situations may occur, for some airframe designs, where damage or a combination of damages that lead to partial local loss of stiffness or increased mass may lead to flutter failures. The simulation

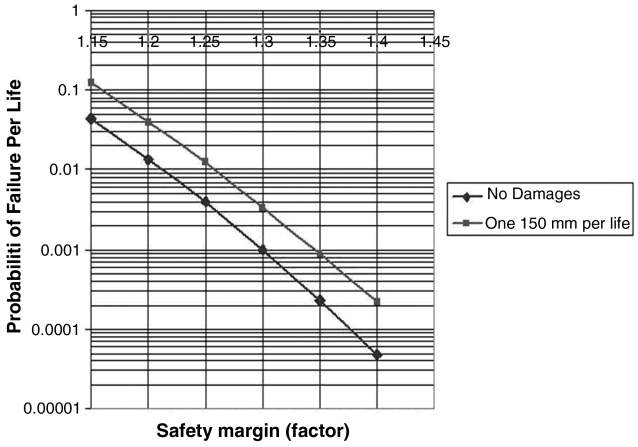

Fig. 18 Flutter POF vs safety margin (factor).

capabilities developed for this work and described previously can be used to identify such cases and to study them, as well as the consequences and tradeoffs for design and maintenance.

VI. Conclusions

A method for quantifying the reliability and damage tolerance of aircraft composite structures due to flutter in the presence of multiple uncertainties was presented in this paper. Automated rapid simulation tools for predicting flutter speeds for composite airframes subject to multiple uncertainties (our VATM capabilities) serve a key role and are used in Monte Carlo simulations. The effectiveness of the method is illustrated on a typical composite aircraft tail/rudder structure. Conclusions of the exploratory studies reported here include the following:

1) Probabilistic methods may be used effectively to quantify the flutter reliability of composite aircraft structures, thus enabling aircraft manufacturers, operators, and flight certification authorities to establish design, maintenance, and service guidelines that reduce life-cycle cost.

2) The inspection interval that insures a reasonably high reliability depends primarily on the statistical characteristics of external loads and flight speeds; damage rates, types, inspection, and repair; and both residual static strength and stiffness of the damaged structure.

3) The most uncertain variables in any probabilistic damage-tolerance design method are damage size and frequency. To obtain in-service data that contain complete descriptions of damage size and frequency, structural locations, inspection methods, and repair used is still a major challenge, but it is of major importance.

4) Additional studies of different structural airframe configurations are required. In particular, horizontal tail/elevator/tab systems, wing/control surface systems, and complete aircraft. Effects of hinge failure and possible failure of internal structure should also be considered. Other modes of failure due to aeroelastic behavior should be studied too, such as dynamic stresses due to gust excitation and the fatigue effects of LCOs. The methodology presented here and the associated simulation tools can be extended to cover all such cases.

Acknowledgments

This work was supported under the Federal Aviation Administration (FAA) Research Grant: Combined Global/Local Variability and Uncertainty in Integrated Aeroservoelasticity of Composite Aircraft. The authors wish to thank the FAA Center of Excellence at the University of Washington (AMTAS) for sponsoring the current research project. Peter Shyprykevich and Curtis Davies were the grant monitors. Larry Ilcewicz's interest and support are gratefully acknowledged. Thanks to the Boeing Commercial Airplane Group for help and support and, at of the University of Washington's Department of Aeronautics and Astronautics, thanks go to Kuen Lin for his vision, guidance, and advice. The authors also thank Paolo Feraboli for valuable discussions on the possible effect of repair on flutter.

References

[1] "*Airworthiness Standards: Transport Category Airplanes*," Federal Aviation Authority, FAR 25.629. Washington, D. C., 2000.

[2] Pettit, C. L., "Uncertainty Quantification in Aeroelasticity: Recent Results and Research Challenges," *Journal of Aircraft*, Vol. 41, No. 5, 2004, pp. 1217–1229. doi:10.2514/1.3961

[3] Lin, K., and Styuart, A., "Probabilistic Approach to Damage Tolerance Design of Aircraft Composite Structures," *Journal of Aircraft*, Vol. 44, No. 4, July–Aug. 2007, pp. 1309–1317. doi:10.2514/1.26913

[4] Schaeffer, H. G., "MSC. Nastran Primer for Linear Analysis," 2nd ed., MSC Software, Santa Ana, CA, 2001.

[5] "ZAERO, Engineers' Toolkit for Aeroelastic Solutions," ZONA Technology, Scottsdale, AZ, 2004.

[6] Chen, P. C., Liu, D. D., and Livne, E., "Unsteady Aerodynamic Shape Sensitivities for Airplane Aeroservoelastic Configuration Optimization," *Journal of Aircraft*, Vol. 43, No. 2, 2006, pp. 471–481. doi:10.2514/1.10007

[7] Chen, P. C., Zhang, Z., and Livne, E., "ZEUS-DO: Design Oriented CFD-Based Unsteady Aerodynamics for Flight Vehicle Shape Optimization," 51st AIAA/ASME/ASCE/AHS/ASC Structures, Structural Dynamics, and Materials Conference, Orlando, FL, AIAA Paper 2010-2720, 12–15 April 2010.

[8] Haftka, R. T., and Yates, E. C., Jr., "Repetitive Flutter Calculations in Structural Design," *Journal of Aircraft*, Vol. 13, No. 7, 1976, pp. 454–461. doi:10.2514/3.58678

[9] Meyer, E. E., "Application of a New Continuation Method to Flutter Equations," 29th Structures, Structural Dynamics and Materials Conference, Williamsburg, VA, AIAA Paper 1988-2350, 18–20 April 1988.

[10] Gordon, J., Meyer, E., and Minogue, R., "Nonlinear Stability Analysis of Control Surface Flutter with Freeplay Effects," *Journal of Aircraft*, Vol. 45, No. 6, 2008, pp. 1904–1916. doi:10.2514/1.31901

[11] Eldred, M. S., Venkayya, V. B., and Anderson, W. J., "New Mode Tracking Methods in Aeroelastic Analysis," *AIAA Journal*, Vol. 33, No. 7, 1995, pp. 1292–1299. doi:10.2514/3.12552

[12] Eldred, M. S., Venkayya, V. B., and Anderson, W. J., "Mode Tracking Issues in Structural Optimization," *AIAA Journal*, Vol. 33, No. 10, 1995, pp. 1926–1933. doi:10.2514/3.12747

[13] Chen, P. C., "A Damping Perturbation Method for Flutter Solution: The *g*-Method," *AIAA Journal*, Vol. 38, No. 8, Aug. 2000, pp. 1519–1524. doi:10.2514/2.1171

[14] Livne, E., "Integrated Aeroservoelastic Optimization: Status and Progress," *Journal of Aircraft*, Vol. 36, No. 1, Jan.–Feb. 1999, pp. 122–145. doi:10.2514/2.2419

[15] Edwards, J. W., and Wieseman, C., "Flutter and Divergence Analysis Using the Generalized Aeroelastic Analysis Method," *Journal of Aircraft*, Vol. 45, No. 3, 2008, pp. 906–915. doi:10.2514/1.30078

[16] Roger, K. L., "Airplane Math Modeling Methods for Active Control Design," *Structural Aspects of Active Controls*, AGARD CP228, Aug. 1977, pp. 4–11.

[17] Karpel, M., "Design for Active Flutter Suppression and Gust Alleviation Using State Space Aeroelastic Modeling," *Journal of Aircraft*, Vol. 19, No. 3, March 1982, pp. 221–227. doi:10.2514/3.57379

[18] Karpel, M., "Sensitivity Derivatives of Flutter Characteristics and Stability Margins for Aeroservoelastic Design," *Journal of Aircraft*, Vol. 27, No. 4, 1990, pp. 368–375. doi:10.2514/3.25281

[19] Mor, M., and Livne, E., "Minimum State Unsteady Aerodynamics for Aeroservoelastic Configuration Shape Optimization of Flight Vehicles," *AIAA Journal*, Vol. 43, No. 11, Nov. 2005, pp. 2299–2308. doi:10.2514/1.10005

[20] Nissim, E., "On The Formulation of The Minimum-State Approximation as a Non-Linear Optimization Problem," *Journal of Aircraft*, Vol. 43, No. 4, July–Aug. 2006, pp. 1007–1013. doi:10.2514/1.17148

[21] Nissim, E., "On the Uniqueness of the Minimum State Representation," *Journal of Aircraft*, Vol. 42, No. 5, Sept.–Oct. 2005, pp. 1339–1340. doi:10.2514/1.15105

[22] Mor, M., and Livne, E., "Minimum State Unsteady Aerodynamic Shape Sensitivities Using Sensitivity of Optimal Solutions to Problem Parameters," *AIAA Journal*, Vol. 45, No. 9, 2007, pp. 2187–2195. doi:10.2514/1.24480

[23] Vanderplaats, G. N., *Numerical Optimization Techniques for Engineering Design*, 3rd ed., Vanderplaats Research and Development, Novi, MI, 2001.

[24] Styuart, A., Mor, M., Livne, E., and Lin, K., "Risk Assessment of Aeroelastic Failure Phenomena in Damage Tolerant Composite Structures," 48th AIAA/ASME/ASCE/AHS/ASC Structures, Structural Dynamics, and Materials Conference, Honolulu, HI, AIAA Paper 2007-1981, 23–26 April 2007.

[25] Selikhov, A. F., and Chizhov, V. M., *Probabilistic Methods in Structural Strength Analysis*, Mashinostroenie Publ. House, Moscow, 1987 (in Russian).

[26] Taylor, J., *Manual on Aircraft Loads*, Pergamon Press, Oxford, NY1965.

[27] Styuart, A. V., Chizhov, V. M., and Legnyov, M. Y., "Extrapolation of Load Exceedance Curves for Estimation of Probability of Aircraft Structural Failure," *Tekhnika Vozdushnogo Flota*, Vol. 635, No. 6,

1998, pp. 27–33 (in Russian).
[28] Rustenburg, J., Skinn, D., and Tipps, D. O., "Statistical Loads Data for Boeing 737-400 in Commercial Operation," U. S. Department of Transportation Rept. DOT/FAA/AR-98/28, Aug. 1998.
[29] Tipps, D. O., Rustenburg, J., and Skinn, D., "Statistical Loads Data for Boeing 767-200ER in Commercial Operation," U. S. Department of Transportation Rept. DOT/FAA/AR-00/10, March 2000.
[30] Rustenburg, J., Skinn, D., and Tipps, D. O., "Statistical Loads Data for Bombardier CRJ100 Aircraft in Commercial Operation," U.S. Department of Transportation Rept. DOT/FAA/AR-03/44, June 2003.
[31] Skinn, D., Tipps, D. O., and Rustenburg, J., "Statistical Loads Data for Md-82/83 Aircraft in Commercial Operations," U. S. Department of Transportation Rept. DOT/FAA/AR-98/65, Feb. 1999.
[32] Rustenburg, J., Skinn, D., and Tipps, D. O., "Statistical Loads Data for the Airbus A-320 Aircraft in Commercial Operation," U. S. Department of Transportation Rept. DOT/FAA/AR-02/35, April 2002.
[33] Acar, E., Kale, A., Haftka, R. T., and Stroud, W. J., "Structural Safety Measures for Airplanes," *Journal of Aircraft*, Vol. 43, No. 1, Jan.–Feb. 2006, pp. 30–38. doi:10.2514/1.14381
[34] Composite Materials Handbook, U.S. Dept. of Defense MIL-HDBK-17-3F, Vol. 3, 17 June 2002.
[35] Brenner, M. J., "Aeroservoelastic Uncertainty Model Identification From Flight Data," NASA TM 2001-210397, July 2001.
[36] Cooper, J. E., "Towards Faster and Safer Flight Flutter Testing," RTO AVT Symposium on Reduction of Military Vehicle Acquisition Time and Cost Through Advanced Modelling and Virtual Simulation, NATO Paper 089, March 2003.
[37] Pickrel, C. R., and White, P. J., "Flight Flutter Testing of Transport Aircraft: In-Flight Modal Analysis," *Proceedings of IMAC 21, the International Modal Analysis Conference* [online], Kissimmee, FL, 2003, http://sem-proceedings.com/21i/sem.org-IMAC-XXI-Conf-s15p06-Flight-Flutter-Testing-Transport-Aircraft-In-flight-Modal-Analysis.pdf [retrieved 2010].
[38] Mevel, L., Goursat, M., Benveniste, A., and Basseville, M., "Aircraft Flutter Test Design Using Identification and Simulation: A SCILAB Toolbox," *Proceedings of 2005 IEEE Conference on Control Applications*, IEEE Publ., Piscataway, NJ, 28–31 Aug. 2005, pp. 1115–1120.
[39] Heeg, J., "Stochastic Characterization of Flutter using Historical Wind Tunnel Data," 48th AIAA/ASME/ASCE/AHS/ASC Structures, Structural Dynamics, and Materials Conference, AIAA Paper 2007-1769, 23–26 April 2007.
[40] "Static Strength Substantiation of Composite Airplane Structure," Federal Aviation Administration Policy Statement PS-ACE100-2001-006, 21 Dec. 2001.
[41] *NESSUS Theoretical Manual, Version 7.0*, Southwest Research Inst., San Antonio, TX, Oct. 2001.
[42] Styuart, A., Demasi, L., Livne, E., and Lin, K., "Probabilistic Modeling of the Aeroelastic Life Cycle for Risk Evaluation of Composite Structures," 49th AIAA/ASME/ASCE/AHS/ASC Structures, Structural Dynamics, and Materials Conference, Schaumburg, IL, AIAA Paper 2008-2300, 2008.
[43] Gary, P. M., and Riskalla, M. G., "Development of Probabilistic Design Methodology for Composite Structures," Federal Aviation Administration, DOT/FAA/AR-95/17, Aug. 1997.
[44] Lin, K. Y., Du, J., and Rusk, D. T., "Structural Design Methodology Based on Concepts of Uncertainty," NASA, CR 2000-209847, Feb. 2000.
[45] Huang, C., and Lin, K. Y., "A Method for Reliability Assessment of Aircraft Structures Subject to Accidental Damage," 46th AIAA/ASME/ASCE/AHS/ASC Structures, Structural Dynamics and Materials Conference, Austin, TX, AIAA Paper 2005-1830, 18–21 April 2005.
[46] Mahadevan, S., and Dey, A., "Adaptive Monte Carlo Simulation for Time Variant Reliability Analysis of Brittle Structures," *AIAA Journal*, Vol. 35, No. 2, 1997, pp. 321–326. doi:10.2514/2.95
[47] Ushakov, A., Stewart, A., Mishulin, I., and Pankov, A., "Probabilistic Design of Damage Tolerant Composite Aircraft Structures," Federal Aviation Administration, Rept. DOT/FAA/AR-01/55, Jan. 2002.

B. Balachandran
Associate Editor